U. of Iowa 67-69

The Magnetospheric Radiation Belt and Tail Plasma Sheet

by

J. H. Piddington*

Department of Physics and Astronomy
University of Iowa
Iowa City, Iowa 52240

November 1967

* Usual Address: C.S.I.R.O. Division of Physics, University Grounds, Chippendale, NSW, Australia

This work was supported in part by the National Aeronautics and Space Administration under contract NsG 233-62.

ABSTRACT

Theories of the origin of the storm-time radiation belt (the ring current) and associated bays and auroras have invoked hydromagnetic flow from the magnetotail on the one hand and flow into the tail on the other. It is shown that both flow patterns occur, the inward flow being the source of energy and driving the major magnetospheric convection pattern. Inward flow is the source of lower energy ($E \lesssim 10$ keV) auroral particles, of the asymmetric or storm-time radiation zone and higher energy ($E \gtrsim 20$ keV) trapped particles, and of the permanent radiation belt itself.

When the asymmetric belt develops sufficient energy density ($\gtrsim 10^{-8}$ erg cm^{-3}) an electric space-charge field develops which changes the plasma convection pattern and ionospheric current system. The following phenomena are explained:

(a) The tail plasma sheet is formed by the outward Hall drift of plasma from the storm-time radiation zone.

(b) On a smaller scale, "bubbles" of plasma from the radiation zone are released into the tail, accounting for the observed "islands" of tail electrons, "spikes" of electrons seen just above the ionosphere, and energetic protons ($\lesssim 300$ keV) which have been seen in the tail.

(c) The storm or bay ionospheric current system (DP1) develops from the quiet-time system (DP2) as a result of the magnetospheric space-charge field and changed ionospheric conductivity caused by auroral precipitation.

(d) Quiet auroral arcs and auroral substorms are due to electron precipitation from regions of low magnetic field strength, where the first invariant (of trapped particles) is lost.

The intermittent ejection of plasma from the radiation belt suggests that the model be termed the "burping radiation belt".

1. INTRODUCTION

Theory has long predicted the development of a belt of trapped energetic particles to explain the main phase of a geomagnetic storm, and observational evidence now confirms its existence [Cahill, 1966, 1967; Frank, 1967]. The belt develops asymmetrically, growing first in the night and evening sectors where it is associated with powerful ionospheric current systems and auroral activity. These are clearly part of one very complex phenomenon.

A phenomenon not generally identified with the ring current or storm-time radiation belt is the permanent belt of Van Allen radiation. The origin of this radiation is not understood, but the evidence is becoming stronger that the storm-time belt represents a rather convulsive development stage of the permanent belt. Thus the origin of the storm-time radiation belt is basic to the understanding of the main magnetospheric processes as well as to some auroral and magnetic phenomena.

The introduction of hot plasma and Van Allen particles into the magnetosphere following magnetic reconnection in a magnetotail has been discussed by Piddington [1960, 1965, 1967a], Axford et al. [1965], Atkinson [1966] and Dungey [1967]. The theory is successful in accounting for energy requirements and in explaining some magnetic

and auroral effects. However, there is disagreement about the form of the equivalent ionospheric current system and its changes during a storm, and different workers have attempted to explain different features of these current systems as independent phenomena. There has also been confusion in the use of auroral data which now reveal a complex family of phenomena having different, although related origins.

The basic feature of the tail reconnection model is flow of plasma with frozen in field from the tail to the corotating magnetosphere. Recently, observational evidence discussed below has cast some doubt on this feature by revealing frequent outward motions into the tail.

It is the purpose of this paper to attempt to reconcile these apparent discrepancies and to show that a single model may explain:

(a) Two basically different equivalent ionospheric current systems,

(b) various auroral precipitation phenomena,

(c) the radiation belts, asymmetrical and symmetrical, and

(d) the ejection of plasma into the tail to form the tail plasma sheet, electron "islands" and "spikes". Following the common proceedure of using a catch phrase to identify a model, we call it the "burping radiation belt".

2. THE EVIDENCE OF PLASMA FLOW FROM THE TAIL

Observational evidence suggests that the storm-time radiation belt develops asymmetrically, with maximum intensity in the evening sector. The theory of its origin from tail plasma depends on a variety of data and these require a brief review before we attempt to extend the model to account also for plasma flow into the tail.

2.1 Equivalent Ionospheric Current Systems

Sea-level magnetic perturbations may be converted to equivalent current systems, which are systems which would explain the perturbations, but are not unique in that respect. The decrease in horizontal intensity at low latitudes is not uniform in longitude and has been interpreted as indicating the development of a storm-time belt strongest in the evening sector [Akasofu, 1967]. Such a development, which is also indicated by the particle data, is consistent with flow inward from the tail.

It is the high latitude equivalent ionospheric current systems which indicate likely flow patterns. These have a variety of forms as well as intensity but may be divided into two types [See Obayashi, 1966]. The magnetic bay or substorm system (or DP1 system) is observed briefly during substorms and is, we believe, a temporary departure from the general flow pattern. It results from a changed

system of electric fields, but also to a large extent from changed ionospheric conductivity caused by auroral precipitation. Its interpretation is therefore difficult and is delayed to a later section, where it is treated as a system which evolves from the normal current system.

The normal current system, which is found during periods of average activity and also at times during the early parts of storms, is shown in Fig. 1a. This DP2 pattern has been derived with small variations by Nagata and Kokubun [1962], Nishida [1967] and others. Although less spectacular than DP1 electrojets, it is the system which flows most of the time and so indicates the usual magnetospheric activity.

A most important point to note in using these data is that they are equivalent current systems. They must be driven by magnetospheric electric fields and so currents must flow down the field lines as well as in the ionosphere. It has been shown [Piddington, 1962] that the sea-level magnetic field caused by the downflowing currents cancels out the effects of ionospheric Pedersen current, so that the equivalent current system is substantially Hall current. The latter is carried by electrons which follow the motions of the magnetic field lines in their magnetospheric interchange motions. Hence these motions are given by simply reversing the current arrows to give the drift arrows V_q in Fig. 1a. It will be

seen that this drift carries the ends of the field lines into the auroral oval (dashed) which defines the cross section of the magnetotail. The polar plot of Fig. 1a may be projected into an equatorial section to give drift V_q shown in Fig. 1b; here drift through the tail is not shown. The power required to maintain these drifts or magnetospheric convection is supplied by frictional interaction with the solar wind [Piddington, 1962, 1964].

This simple interpretation of the equivalent ionospheric current system DP2 introduces a flow pattern of plasma and frozen in field lines to and from the tail and leads to the inward flow model [Piddington, 1967a]. Most other interpretations of the equivalent current systems treat them as real current systems. This overlooks the fact that the real system is part of a hydromagnetic disturbance originating above the magnetosphere and propagating downwards. Such a disturbance cannot propagate freely in the non-conducting atmosphere. In fact, apart from ionospheric Hall current, most high latitude disturbances would cause little or no sea-level disturbance.

2.2 Auroral Morphology

Aurorae are such a complex family of phenomena that their use in developing a theory of the magnetosphere is difficult. They may, however, be divided into several different types according to zones of occurrence and other properties [Piddington, 1965]. Only Zone II or discrete visual auroras are required for the present

discussion and these define Feldstein's "auroral oval" which is identified with the boundary of the magnetotail as it crosses the ionosphere. This boundary is shown in Fig. 2 for average conditions, and the identification is confirmed by a number of phenomena: the boundary of trapped fast particles, some hydromagnetic waves, "tail spikes" and magnetic conjugate experiments [Piddington, 1967a,b].

Also shown in Fig. 2 is the auroral oval and presumed tail section during a great magnetic storm. If this interpretation is correct then the magnetic flux in the tail doubles from its average value of $\sim 7 \times 10^{16}$ gauss cm^2 and the magnetic energy stored within a distance of 100 earth radii (R_E) exceeds 10^{23} erg. This energy provides a store which is adequate to supply the storm-time ring current, auroral and ionospheric dissipation. However, if the energy is to be used in this way, then the mechanisms involved are automatically defined.

The magnetotail energy is the only apparent source capable of providing the requirements of the storm-time radiation belt. It may be utilized only by the reconnection of magnetic field lines from the northern and southern hemispheres across the neutral sheet, and their subsequent withdrawal from the tail. Such a flow of field lines and plasma from the tail is also consistent with the form of drift pattern V_q shown in Fig. 1. This flow pattern is thought to continue during storms as well as during periods of quiet. During

substorms and during isolated bays the model provides a second system of drifts and currents which, when combined with DP2 and changes in ionospheric conductivity, give the substorm or bay or DP1 system.

An important feature of the theory is the massive precipitation of electrons to provide visual auroras and to increase ionization in the region 90-120 km in which most of the Cowling conductivity is developed. For the present discussion, however, we are more concerned with particles which remain trapped. In the tail plasma sheet there is a good supply of particles of energy $\lesssim$ 1 keV, and in the neutral sheet these are trapped in a field of strength about 1 γ [Speiser and Ness, 1967]. Following reconnection of more field lines, these particles are moved into the corotating magnetosphere to say $5R_E$ and to a region where the field strength exceeds 100 γ so that the particles attain energies of $\lesssim$ 100 keV, with some at higher energies [Sakurai, 1966]. These particles provide the asymmetrical radiation zone and other phenomena. They account for the observations of Konradi [1967] of protons of energy > 100 keV in the day sector and his interpretation of injection in the night sector and westward drift.

The asymmetrical radiation has been drawn in magnetospheric equatorial section [Piddington, 1967a, Fig. 3] and is shown in ionospheric projection (projection being along the field lines) in

Fig. 3 below. The auroral oval is shown and the DP2 drift pattern (V_q of Fig. 1a) is now modified to that shown by the arrows V_p. This is a result of the addition of a new plasma drift V_s, caused by an electric space-charge field. On entering the corotating magnetosphere protons drift westward at a rate proportional to their energy, about 1 radian per hour for 15 keV ions. This places the asymmetric proton belt in the dusk hemisphere as shown. Trapped electrons, which appear to have a lower energy density, will drift eastward but at a lower rate than the protons. The drift lines V_q are sketched at right angles to the gradient of electric potential caused by these accumulations of space charge.

3. THE RELEASE OF PARTICLES INTO THE TAIL

The magnetotail has an overall extent perpendicular to the neutral sheet of about 40 R_E, but the neutral sheet itself has a thickness of only 0.1 - 1 R_E [Speiser and Ness, 1966]. This thin sheet lies within a broad region of magnetic field depression and plasma enhancement called the tail plasma sheet, and the two sheets are shown schematically in Fig. 4. The plasma sheet has thickness varying from 4 R_E to about 12 R_E [Bame et al., 1967], averaging $\sim$ 30 times that of the neutral sheet.

3.1 Observational Data

Hones et al. [1967] have studied the tail plasma sheet at geocentric distances $\sim$ 17 R_E and found that both the lower energy

(300 eV - 20 keV) and higher energy (> 45 keV) electrons disappear and reappear in a characteristic sequence shown in Fig. 5a by the plot P. Also shown is a geomagnetic negative bay in the form of a plot of the X component from a station near the same magnetic longitude. At the start of the bay a gradual decrease in P shows that the plasma sheet disappears from the vicinity of the satellite within a period 1/2 - 1 hour. At the time of bay minimum the plasma sheet reappears abruptly at full intensity. In addition to temporary disappearances of the tail plasma sheet, Hones et al. report many temporary appearances. These are usually abrupt and occur during a negative bay; the subsequent decay is much slower.

It does not seem possible to account for the sudden appearances of tail plasma, either temporary or permanent, in terms of diffusion from the neutral sheet. Nor is it possible to explain Fig. 5a in terms of activity in the distant tail and subsequent flow of plasma towards the earth; this would give an increase which would either be sustained or followed by a decrease. As suggested by Hones et al., it seems that at the onset of a bay plasma moves from the vicinity of the satellite (at $\sim 17\ R_E$) towards the earth, and later returns. Extending these considerations, one must conclude that it is most unlikely that the tail plasma sheet could be formed as a direct result of any processes within the tail. Its great extent makes this unlikely, as does the quality of its plasma which is generally much "hotter" than the particles causing discrete auroras.

It would seem that the "plasma appearances" of Hones et al. must be identified with the "islands" of energetic electrons and depressed magnetic intensity seen in the tail [Anderson and Ness 1966 and others] and with the "spikes" of electrons seen at lower levels by Fritz and Gurnett [1965] and McDiarmid and Burrows [1965] and shown in Fig. 2. These phenomena occur far from the tail neutral sheet (the auroral oval) and so could hardly originate within the tail.

Finally we have evidence from several quarters of outward travelling effects in the tail. Magnetic disturbances in the tail are seen to follow negative bays [Heppner et al., 1967]. Armstrong and Krimigis [1967] have observed bursts of protons of energy > 300 keV which correlate with negative bays and appear to stream away from the earth. Rothwell [1967] has shown that the electrons forming the "islands" move similarly.

We must conclude that, even though the most important movement of field lines and plasma is inwards from the tail, during the relative brief periods of negative bays plasma is somehow released again into the tail. Swift [1964, 1967 a,b] has suggested a flute instability on the outer boundary of the ring current; this involves the development of an electric field of the type shown in Fig. 3. Taylor and Hones [1965] have proposed a magnetospheric convection model which provides outward drifts, but it is not clear how this

model is driven or from where the necessary power is derived.

3.2 Particle Drifts in the Radiation Belt

In the closed magnetosphere two particle drift motions are superimposed on the general convection pattern of Fig. 16. These are the drifts of energetic electrons and protons caused by the gradient of the magnetic field $\underline{B}$, and the Hall drift of all particles caused by any additional space-charge field $\underline{E}$. These drifts are given by

$$\underline{U} = \frac{\underline{B}}{B^2} \times \left(-\underline{E} + \frac{\mu}{e} \nabla B \right) , \qquad (1)$$

where μ and e are the magnetic moment and charge (emu) of the particle. There is also a drift due to motions of particles along field lines but in the present order-of-magnitude model this is neglected.

Energetic particles in a radiation zone will drift so as to create a westward electric current and in a symmetric zone this is a stable ring current. In the asymmetric part of the zone shown in Fig. 3 protons drift westward and electrons eastward to create electric space charge as shown, and this in turn drives ionospheric currents in the manner discussed by Fejer [1961] and others. The space charge has other effects and so we make an order of magnitude estimate of the electric field.

Two geometric factors are required to define the asymmetric zone of Fig. 3: its thickness ℓ_a in the direction perpendicular to

the equatorial plane and its boundary thickness ℓ_b which relates the field gradient to the average field B_o by the equation $B_o = \ell_b \nabla B$. We also note that in moving along the field lines a magnetic field B_o in the magnetosphere transforms to a field $s^2 B_o$ in the ionosphere and an electric field by a factor s. A strip 1 cm wide in the ionosphere (along a parallel of latitude) has an effective or Cowling conductivity Σ_3 integrated vertically through the ionosphere. This strip projects into an equatorial width of s cm and the circuit or (ring current) cross-sectional area is $s\ \ell_a$.

Let drift motions create an electric field E_m in the magnetosphere, then this will project to a field sE_m and drive an ionospheric current

$$J = \Sigma_3\ s\ E_m \quad . \tag{2}$$

In the magnetosphere the space charge $N_i e$ is carried by ions of density N_i with drift velocity $\mu \nabla B / eB_o$ to carry the same current, now given by

$$J = W_i\ \nabla B\ B_o^{-2}\ s\ \ell_a\ , \tag{3}$$

where W_i is the ion energy density due to transverse motion, so that $W_i = \mu\ B_o\ N_i$. Replacing ∇B by B_o / ℓ_b and eliminating J we have

$$E_m = \frac{W_i \ell_a}{\Sigma_3 B_o \ell_b} \qquad (4)$$

During a magnetic storm, Frank [1967] has observed a proton energy density $\sim 10^{-7}$ erg cm^{-3}. A large part of this is probably represented by the symmetrical belt, but we will assume that 10 per cent is asymmetrical. We put $B_o = 1.5 \times 10^{-3}$ gauss, corresponding to an L value for a dipole field of about 6 (or a smaller value for an inflated magnetosphere). The value of Σ_3 for the night ionosphere in the absence of auroral particles is about 2×10^{-9} emu [Johnson, 1965] and if we put $\ell_a \sim \ell_b$, then we find $E_m \sim 3 \times 10^3$ emu. The corresponding drift velocity found by substituting E_m for E in equation (1) is ~ 20 km sec^{-1} or 11 R_E per hour.

The characteristic time for a bay or substorm is 1 - 3 hours and with the above drift velocity a major redistribution of magnetospheric plasma must occur. This is discussed in the following section. Other effects which result from the polarization field are ionospheric currents, the development of a full ring current and of the Zone I auroras and finally the development of the auroral substorm.

3.3 The Origin of the Tail Plasma Sheet and Islands

The electric space-charge field E_m is directed eastward and the plasma drift caused by this field is outwards in the meridian

planes. This is shown by the arrows V_s in Figs. 1b and 3 and the arrows F_2 in Fig. 4. In these figures the flow V_s modifies and, in the midnight sector, directly opposes the general flow pattern denoted by V_q (Figs. 1a, 1b) and by F_1 in Fig. 4. The latter may be identified with auroral motions and Hall current (the reverse of the electron Hall drift) in the polar cap; a reasonable value for disturbed conditions is $\lesssim 0.5$ km sec^{-1} [Cole, 1963]. This drift, when projected into the magnetosphere and increased by the factor $s \sim 17$, has a value $\lesssim 9$ km sec^{-1}, or less than half the drift due to E_m.

We concluded that when the asymmetric portion of the storm-time radiation belt attains an energy density of about 10^{-8} erg cm^{-3}, the drift of plasma inwards from the tail is reversed. The flow F_2 of Fig. 4 replenishes the tail plasma sheet and, furthermore, this replenishment is with particles of energy typically $\gtrsim 20$ keV. Particles arriving from the tail and providing discrete (Zone II) auroras are typically $\lesssim 10$ keV. It is only after they have been carried into the storm-time radiation zone and subjected to betatron acceleration that they attain the higher energy typical of Zone I [See Piddington 1967a,b].

In discussing convective motions in a closed magnetosphere where $\frac{\partial \underline{B}}{\partial t} = 0$ everywhere, we may assume motion of frozen in field

lines and the development of a space-charge field $\underline{E}$ to balance the field $\underline{V} \times \underline{B}$ seen by the moving plasma. There seems to be no way to distinguish between these situations. With a diminishing magnetotail flux, however, we must assume flow of lines from the tail and in general this flow (V_q) is accompanied by plasma. With the demonstrated development of the space-charge field E_m a new situation arises: the field and plasma are decoupled and field lines may continue to move inwards while plasma moves outwards. In this way the tail plasma sheet is created without involving the creation of more tail flux near the midnight sector.

In Fig. 3 we have sketched an asymmetrical radiation belt occupying a quadrant. If reconnection in the tail occurs at random then we might expect to find wider belts and narrower belts. A belt extending only a few degrees in longitude will become polarized and will drive a very localized ionospheric current system. It will also cause a localized ejection of material into the tail and this is proposed as the mechanism causing the tail "islands" of energetic electrons and depressed magnetic field [Anderson and Ness, 1966]. It would also account for the electron "spikes" seen by Fritz and Gurnett [1965] and McDiarmid and Burrows [1965] and the transitory appearances of tail plasma particles $E > 45$ keV seen by Hones et al. [1967].

The escape of particles of energy ~ 300 keV is not so simply explained, because their drift is determined almost entirely by magnetic field gradients. However, these will be large and localized in the regions of tail islands and spikes. If the energy density of the plasma in the radiation belt is 10^{-7} erg cm^{-3} [Frank, 1967], then the magnetic field strength required to give an equal energy density is 1.6×10^{-3}, which is approximately the value of the undistrubed field in the region concerned ($L \sim 6$). The plasma is thus capable of creating a near magnetic vacuum and any extra plasma in a localized region (asymmetrical zone) will experience a large electric field (E_m in equation 4) and a large outward drift E_m/B_o. This is essentially the flute instability which Chang et al. [1965] have suggested as a possibility in a region of low enough ionospheric conductivity Σ_3. With a very low value of B_o the plasma "bubble" will drift rapidly into the tail and may carry energetic particles such as those seen by Armstrong and Krimigis [1967]. This bubble model also allows electrons of energy $E \gtrsim 20$ keV to reach the tail without being decelerated; the reason is that the magnetic moment is not conserved.

It is of interest to estimate the length of the plasma tail, as distinct from the magnetic tail which extends for some hundreds of R_E. The estimate is based on the assumption that all magnetic field lines in the plasma sheet are connected across the neutral sheet and have begun to contract back towards the earth.

Other field lines are being drawn into the tail and 40 keV electrons released into these lines would be lost. Consider a slab of tail plasma in the midnight meridian (x z plane of Fig. 4) of thickness 1 cm. If the tail field strength is 15 γ and the plasma sheet has a semi-thickness of 2 R_E, then the flux into one half of this slab is $\sim 2 \times 10^5$ gauss cm^2. The field strength across the neutral sheet is less than 1 γ [Speiser and Ness, 1966] so that the length of the plasma sheet is more than 30 R_E. Near the dawn side of the tail the plasma sheet has a thickness of $\sim 10R_E$ and the field perpendicular to the neutral sheet is 1 - 4 γ. The plasma tail in this region will have a length of between about 20 R_E and 75 R_E.

4. OTHER PHENOMENA

The introduction of energetic particles to form an asymmetrical radiation zone shown in Fig. 3 must lead to three other effects:

(a) The development of a symmetrical radiation belt

(b) The development of a new ionospheric current system

and

(c) New patterns of auroral precipitation.

4.1 The Origin of the Radiation Belt

Following reconnection of magnetic field lines in the tail, these lines and their share of plasma from the tail plasma sheet move into the corotating magnetosphere as shown by the paths in Fig.1b.

Particles which penetrate more deeply experience more betatron acceleration and as seen above some may attain energies of a few hundred keV. This plasma is distributed initially around the night side of the auroral oval or tail boundary shown in Fig. 2.

More energetic particles now develop a new drift due to the magnetic field gradient, and for energies $\gtrsim$ 20 keV this drift exceeds the general convection of the cold plasma. These particles move approximately along parallels of latitude and because of their spread in velocity and other factors they develop into a complete ring. In Fig. 5b are shown the two main zones of auroral precipitation [Piddington, 1965] which were isolated not only on the basis of a spatial separation but also because of the different properties of the precipitated particles. Zone II is the auroral oval, where large fluxes of softer ($E \lesssim 10$ keV) electrons are precipitated. Zone I is the high-latitude portion of a radiation zone formed in the above manner by the harder ($E \gtrsim 20$ keV) protons and electrons. Particles are precipitated from this zone, the major loss being in the morning sector. Particles in the semi-permanent radiation zone on the equatorward side of Zone I have the same origin but suffer fewer losses.

The growth of this radiation belt, as revealed by the main phase decrease of a geomagnetic storm (D_{st}), is shown as the lower curve of Fig. 6. At time t = 0 the magnetosphere is being inflated

by flow inwards from the tail which continues until a substorm or bay starts and releases some plasma back into the tail. During the bay the outer part of the radiation zone is lost and there is a large decrease in the high-latitude boundary of trapped electrons of $E > 45$ keV (the electrons so lost replenish the tail plasma sheet). This effect is illustrated by the middle curve of Fig. 6; the upper (hatched) part of the figure isdescribed in section 4.3.

The temporary loss of plasma in the rear of the magnetosphere will explain the failure by Akasofu [1967] to detect the storm belt in this region.

4.2 The Origin of Negative Bays

The classical stormtime equivalent ionospheric current system [see, for example, Obayashi, 1966] has four current cells. In addition to two cells which somewhat resemble those of Fig. 1a, there are two lower latitude cells, an anticlockwise cell centred in the early morning and a clockwise cell opposite. These cells seem to compress the DP2 cells (Fig. 1a) into the polar cap and to create electrojets along the auroral oval, westward in the early morning sector and eastward in the afternoon sector. Sometimes the latter is weak or absent and the main feature is a westward jet extending at least from dawn to midnight. This is the DP1 system or substorm current system, which gives rise to the common negative bay.

An explanation of the four-cell current system has been given in terms of an asymmetrical ring current in the night or late evening sector [Fejer, 1961; Cummings, 1966 and others]. Objections to this model are, first that it does not take account of the very large ($\gtrsim$ 1000) and localized changes in the night-time conductivity of the ionosphere caused by auroral precipitation and, second, that a model of the real ionospheric current system is compared with an equivalent ionospheric current derived from sea-level magnetic perturbations.

The model now proposed comprises the two high-latitude Hall current cells similar to those of Fig. 1a, together with two low-latitude Hall current cells driven by the polarized asymmetrical radiation belt. In each cell Pedersen current also flows, but its sea-level magnetic effect, when combined with that due to current flowing up and down field lines, is small. The complete current pattern from these two sources is just the reverse of the drift pattern $V_p + V_s$ of Fig. 3 and so we do not require an additional diagram to show its general form.

The electric field of equation (4), for an asymmetric radiation zone of energy 10^{-8} erg cm^{-3}, has a value $\sim 5 \times 10^{4}$ emu when projected into the ionosphere. Combined with the value of conductivity given above we find $J \sim 10^{-4}$ emu per cm strip and the resulting

sea-level magnetic perturbation is only about 100 γ. This is an order of magnitude less than the observed perturbations, in spite of the fact that the electric field gives outstanding values of drift velocity both in the magnetosphere and in the ionosphere.

The amount of auroral precipitation required to provide a weak arc provides more than 10^{11} electrons cm^{-2} sec^{-1} and will increase the ionospheric conductivity by several powers of 10. This will cause an increase in the ionospheric current, although not in the same proportion because of the limit set by the conductivity away from the auroral arc. The main effect will be a concentration of current into the narrow, highly conducting auroral arc. Lack of precipitation near dusk will result in a single westward arc in the early morning sector.

4.3 Auroral Arcs and Substorms

The two major features of discrete visual auroras are the homogeneous arc and the auroral substorm [Akasofu, 1966]. The former has a ribbon-like structure, extending several thousand kilometres along the auroral oval, yet having a width of only a few hundred metres. There may be several arcs in existance at one time, separated by about 0.3 degrees of latitude and providing a stable pattern which may endure for an hour or more. At the onset of an auroral substorm the luminosity in the midnight sector spreads from

the arc at lowest latitude towards the pole. This is shown in Fig. 6, the hatched area representing the north-south extent of the illumination plotted against time. This activity is confined initially to the midnight sector, but soon the poleward bulge propagates eastward and westward along the pre-existing arcs.

Auroral precipitation has been explained in terms of accelerated magnetic reconnection in the tail and the "dumping" of plasma moving in from the tail [Piddington, 1967a]. This is the most likely origin of the lower energy ($E \lesssim 10$ keV) particles responsible for rapidly fluctuating auroral forms and associated with negative bays of abrupt or rapid onset.

The precipitation of higher energy ($E \gtrsim 20$ keV) electrons appears to be a different, although related, phenomenon [Piddington, 1965]. Such particles and the auroral illumination caused by them were observed by O'Brien [1964] and we identify these with at least some quiet arcs. Observed at a level of about 1000 km, the striking feature about this precipitation event was that the flux of precipitating electrons increased until it equalled but never exceeded the flux of trapped particles.

This phenomenon and the substorm may be explained in terms of the plasma from the asymmetrical radiation belt drifting under the influence of the electric space charge field E_m. This

drift is outwards towards the tail in the night sector as shown in Fig. 3. The current forming the tail neutral sheet flows from the dawn to the dusk side and somewhere between the inner boundary and the corotating magnetosphere there may be a region of zero magnetic field. Plasma particles entering this region are no longer trapped, the first invariant is no longer conserved and the velocity distribution becomes isotropic and remains so in spite of precipitation losses. The width of the precipitation region in the ionosphere is not determined by the dimensions of the region of zero field, but rather by the change in geomagnetic latitude across the region where trapping is lost. The minimum value of this dimension is determined by the gyro diameter of the electrons. Projected into the ionosphere this is only a few tens of metres. Thus the model explains the isotropy of the electrons above the ionosphere and the narrowness of the auroral arc.

Outward drift of the plasma across the field lines provides a continuous source of electrons for precipitation. When the field E_m becomes large the drift increases and a wide band in the ionosphere is connected to a region where the particle flux is isotropic. This is the auroral substorm of Fig. 6 and is accompanied by a marked drop in the latitude of the outer boundary of trapped electrons as shown by the middle curve. As shown in Fig. 3 the outward drift V_s changes into a westward drift in the dusk zone and into an eastward

drift in the early morning zone. This corresponds to the breakup stage of the substorm.

Finally we consider the simultaneous formation of two or more arcs. These are interpreted as precipitation from two or more regions of weak magnetic field, corresponding to a series of hydromagnetic compression waves near the boundary of the corotating magnetosphere.

ACKNOWLEDGEMENTS

I should like to thank Dr. James Van Allen for the hospitality of his department during the course of this work.

This work was supported in part by the National Aeronautics and Space Administration under contract NsG 233-62.

REFERENCES

Akasofu, S.-I., Electrodynamics of the Magnetosphere: Geomagnetic Storms, Space Sci. Rev. 6, 21 (1966).

Akasofu, S.-I., Growth of the Storm-Time Radiation Belt and the Magnetospheric Substorm, Preprint, 1967.

Anderson, K. A., and N. F. Ness, Correlations of Energetic Electrons and Magnetic Fields on the IMP-1 Satellite, J. Geophys. Res. 71, 3705 (1966).

Armstrong, T. P., and S. M. Krimigis, Observations of Protons in the Magnetosphere and Magnetotail, Univ. of Iowa Rep. 67-15 (1967).

Atkinson, G., A Theory of Polar Substorms, J. Geophys. Res. 71, 5157 (1966).

Axford, W. I., H. E. Petschek, and G. L. Siscoe, Tail of the Magnetosphere, J. Geophys. Res. 70, 1231 (1965).

Bame, S. J., J. R. Asbridge, H. E. Felthauser, E. W. Hones, and I. B. Strong, Characteristics of the Plasma Sheet in the Earth's Magnetotail, J. Geophys. Res. 72, 113 (1967).

Cahill, L. J., Inflation of the Inner Magnetosphere during a Magnetic Storm, J. Geophys. Res. 71, 4505 (1966) and NATO Symposium, Freising, Germany (1967).

Chang, D. B., L. D. Pearlstein, and M. N. Rosenbluth, On the Interchange Stability of the Van Allen Belt, J. Geophys. Res. 70, 3085 (1965).

Cole, K. D., Motions of the Aurora and Radio Aurora, Planet. Space Sci. 10, 129 (1963).

Cummings, W. D., Asymmetric Ring Currents and the Low Latitude Disturbance Daily Variation, J. Geophys. Res. 71, 4495 (1966).

Dungey, J. W., The Reconnection Model of the Magnetospheric Tail, NATO Symposium, Freising, Germany (1967).

Fejer, J. A., The Effects of Energetic Trapped Particles on Magnetospheric Motions, Canadian J. Phys. 59, 1409 (1961).

Frank, L. A., On the Extraterrestrial Ring Current During Geomagnetic Storms, J. Geophys. Res. 72, 3753; also NATO Symposium, Freising, Germany (1967).

Fritz, T. A., and D. A. Gurnett, Diurnal and Latitude Effects Observed for 10 keV Electrons at Low Satellite Altitudes, J. Geophys. Res. 70, 2485 (1965).

Heppner, J. P., M. A. Sugiura, T. L. Skillman, B. S. Ledley, and M. Campbell, NASA Publ. X-612-67-150 (1967).

Hones, E. W., J. R. Ashbridge, S. J. Baure, and I. B. Strong, Outward Flow of Plasma in the Magnetotail Following Geomagnetic Bays, Los Alamos Sci. Lab. Rep. LA-DC-8549 (1967).

Johnson, F. S., Satellite Environment Handbook (Stanford University Press, 1965).

Konradi, A., Proton Events in the Magnetosphere Associated with Magnetic Bays, J. Geophys. Res. 72, 3829 (1967).

McDiarmid, I. B., and J. R. Burrows, Electrons Fluxes at 1000 Kilometers Associated with the Tail of the Magnetosphere, J. Geophys. Res. 70, 3031 (1965).

Nagata, T., and S. Kokubun, An Additional Geomagnetic Daily Variation in the Polar Region, Rep. Ionosph. Res. Japan 16, 256 (1962).

Nishida, A., Geomagnetic DP2 Fluctuations, Inst. Space Aeronaut, Sec. Univ. Tokyo, Preprint (1967).

Obayashi, T., The Interaction of Solar Plasma with Geomagnetic Field Disturbed Conditions, Belgrade Symposium (1966).

O'Brien, B. J., High Latitude Geophysical Studies with Injun 3, (3) Precipitation of Electrons, J. Geophys. Res. 69, 13 (1964).

Piddington, J. H., Geomagnetic Storm Theory, J. Geophys. Res. 65, 93 (1960).

Piddington, J. H., A Hydromagnetic Theory of Geomagnetic Storms, Geophys. J. Roy. Astron. Soc. 7, 183 (1962).

Piddington, J. H., Geomagnetic Storms, Auroras and Associated Effects, Space Sci. Rev. 3, 724 (1964).

Piddington, J. H., The Magnetosphere and its Environs, Planet Space Sci. 13, 363 (1965).

Piddington, J. H., The Morphology of Auroral Precipitation, Planet. Space Sci. 13, 565 (1965).

Piddington, J. H., A Theory of Auroras and the Ring Current, J. Atmos. Terr. Phys. 29, 87 (1967a).

Piddington, J. H., The Growth and Decay of the Geomagnetic Tail, N.A.T.O. Conference, Freising, Germany (1967b).

Rothwell, P., Birkeland Symposium (1967).

Sakurai, K., Instability in the Magnetospheric Tail and Acceleration of Auroral Electrons, Rep. Ionosph. Space Res. Japan 20, 49 (1966).

Speiser, T. W., and N. F. Ness, The Neutral Sheet in the Geomagnetic Tail, J. Geophys. Res. 72, 131 (1967).

Swift, D. W., The Connection Between the Ring Current Belt and the Auroral Substorm, Planet. Space Sci. 12, 945 (1964).

Swift, D. W., Possible Consequences of the Asymmetric Development of the Ring Current Belt, Planet. Space Sci. 15, 835 (1967a).

Swift, D. W., The Possible Relationship Between the Auroral Breakup and the Interchange Instability of the Ring Current, Planet. Space. Sci. 15, 1225 (1967b).

Taylor, H. E., and E. W. Hones, Adiabatic Motion of Auroral Particles in a Model of the Electric and Magnetic Fields Surrounding the Earth, J. Geophys. Res. 70, 3605 (1965).

CAPTIONS

FIGURE 1 The "normal" equivalent ionospheric current system and the corresponding drift motions.
(a) The current system DP2 [after Nagata and Kokubun, 1962] is shown by the arrows j. If this is Hall current then the convection or interchange motion is shown by the arrows V_q. The tail section is outlined by dashes.
(b) A projection into the equatorial plane of the convection pattern V_q. Drift within the corotating magnetosphere is shown but not drift in the tail. V_s is a temporary reverse drift which dissipates the midnight sector of the storm radiation belt.

FIGURE 2 A projection in the northern ionosphere of some phenomena which may delineate the magnetotail boundary. The full line is for average conditions and traces Feldstein's auroral oval, the outer boundary of trapped radiation and certain hydromagnetic disturbances. The expanded storm-time oval is shown by wavy lines.

FIGURE 3 An ionospheric projection showing the auroral oval and the modified drift V_p through the tail. An asymmetrical ring current or radiation zone is shown (hatched) and some possible developments comprising electric space charge and Hall drift V_s caused by the new electric field system.

FIGURE 4 A schematic diagram of that part of the magnetotail lying within $\sim 20\ R_E$ and containing the plasma sheet (semi-thickness $2 - 6\ R_E$) and magnetic "neutral" sheet. The radiation zone is shown in cross section, and also the inward (F_1) and outward (F_2) plasma flow.

FIGURE 5 (a) A plot of a geomagnetic negative bay (X) and the corresponding slow disappearance and abrupt reappearance of tail electrons (E > 45 keV) at 17 R_E (after Hones et al., 1967).

(b) A schematic representation of the two principal auroral zones. Zone II is the auroral oval defined by the occurrence of discrete visual auroras (shown under average conditions of disturbance). Zone I is for mantle auroras and is also the outer part of the storm-time radiation zone which extends down to latitudes < 50°. Zone III is the polar cap where various precipitation events occur.

FIGURE 6 A schematic diagram of a pair of auroral substorms plotted in Universal Time and Invariant Latitude Λ; these substorms occur while the auroral oval is expanding. Also shown is the outer limit of the trapping boundary of electrons E > 45 keV and the irregular growth of the ring current.

G67-969

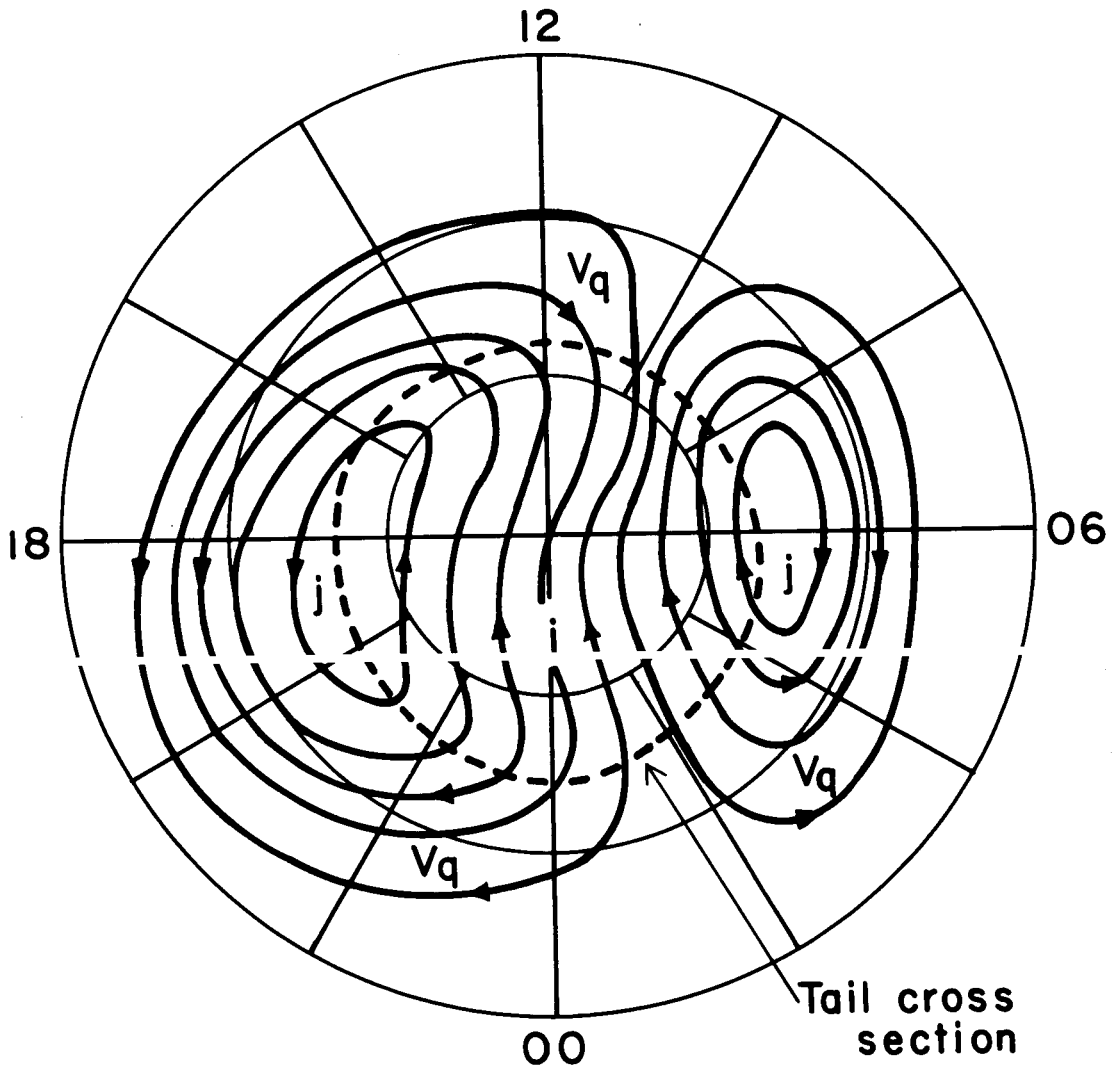

Fig. 1a

G67 – 981

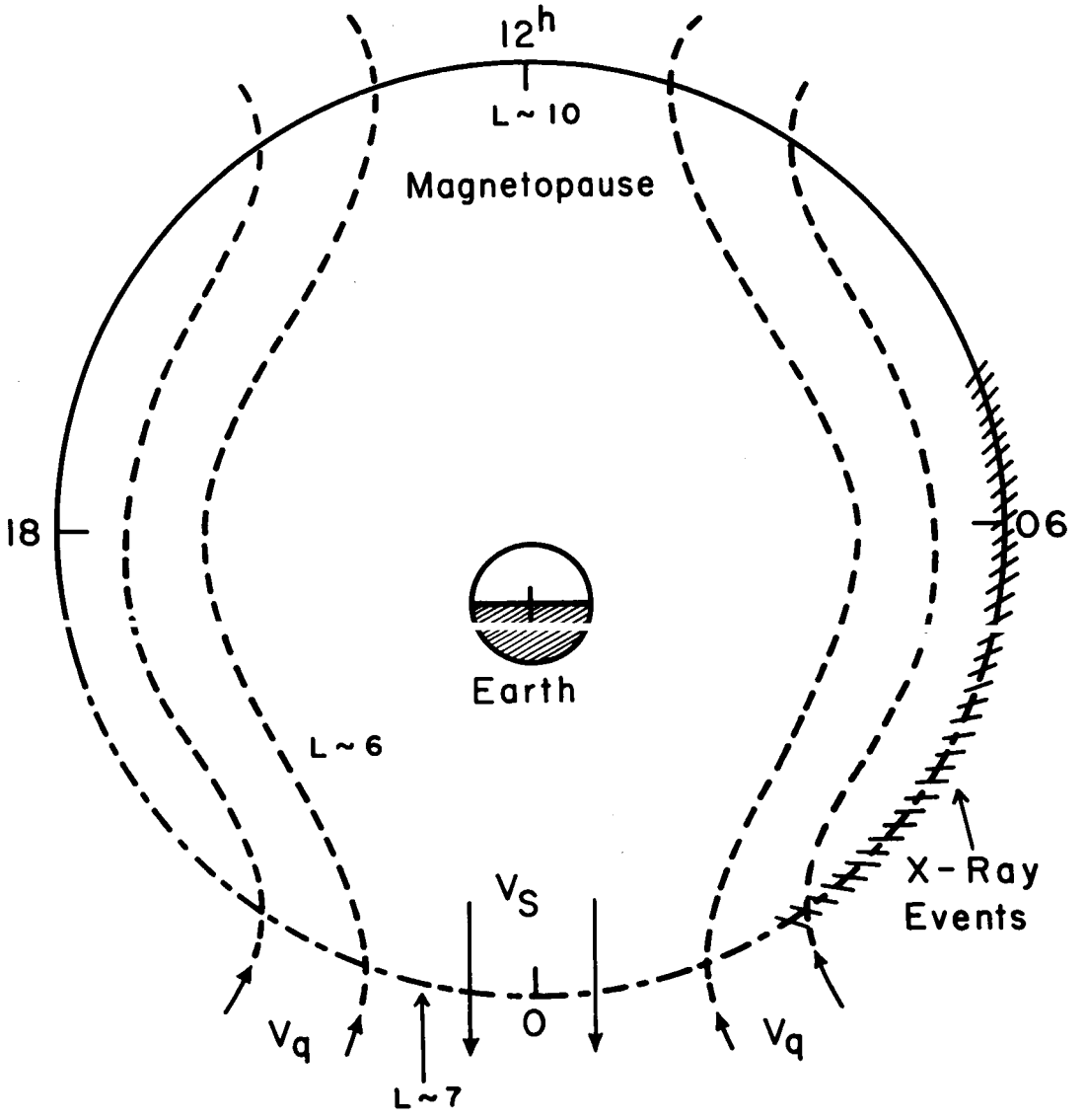

Fig. 1b

G67-982

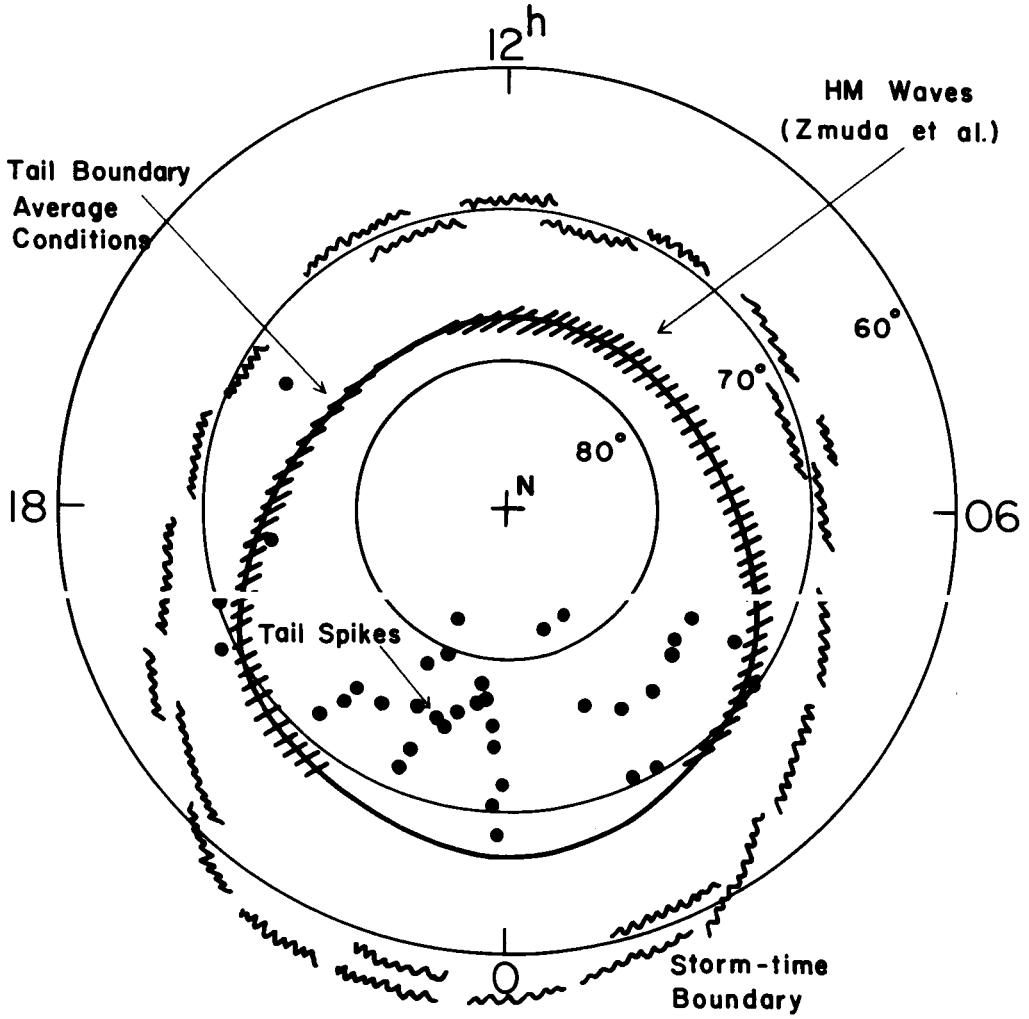
12h
HM Waves
(Zmuda et al.)
Tail Boundary
Average
Conditions
60°
70°
80°
N
18
06
Tail Spikes
Storm-time
Boundary
0

Fig. 2

G67-968

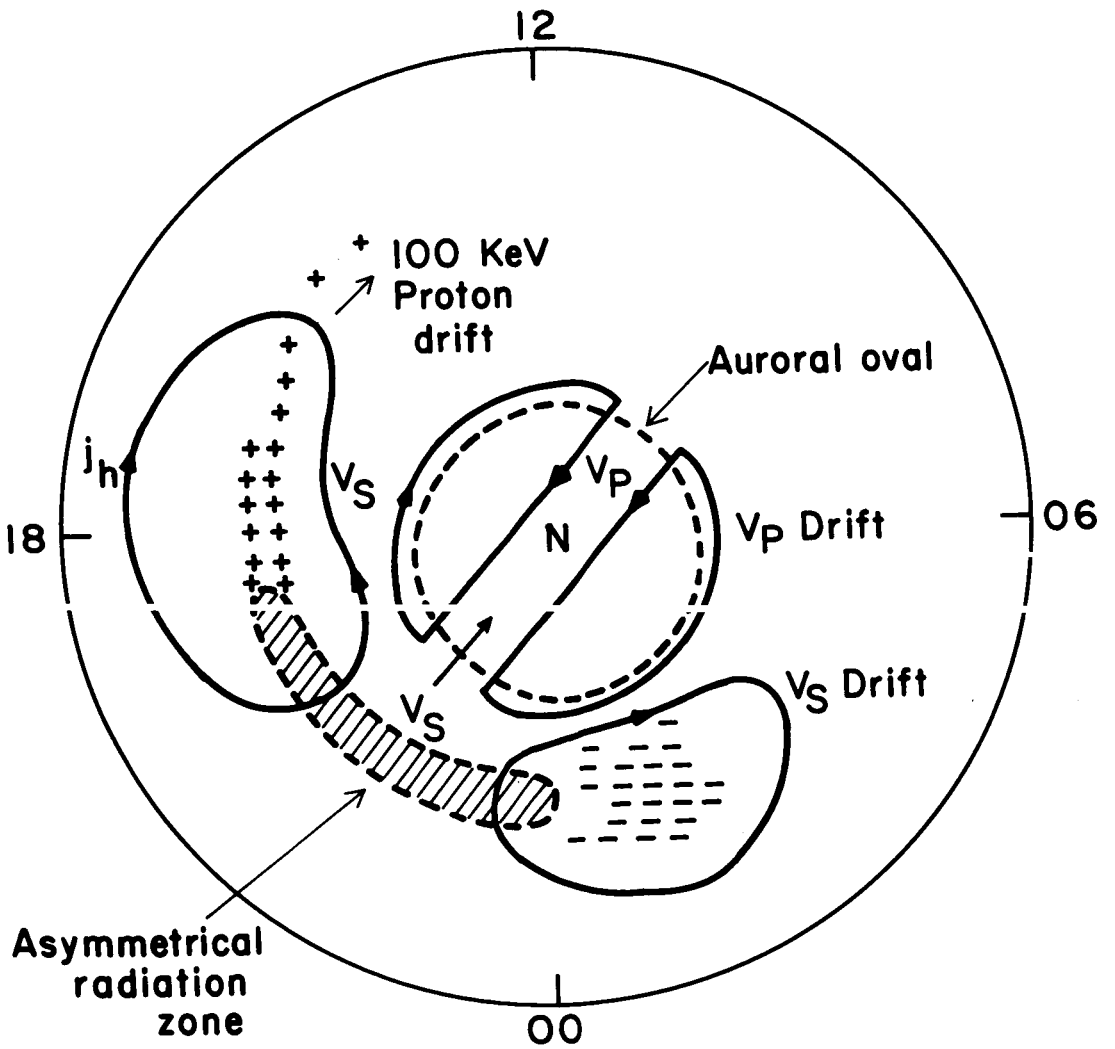
12
18
06
00
100 KeV
Proton
drift
Auroral oval
j_h
V_S
V_P
N
V_P Drift
V_S Drift
V_S
Asymmetrical
radiation
zone

Fig. 3

G67-1033

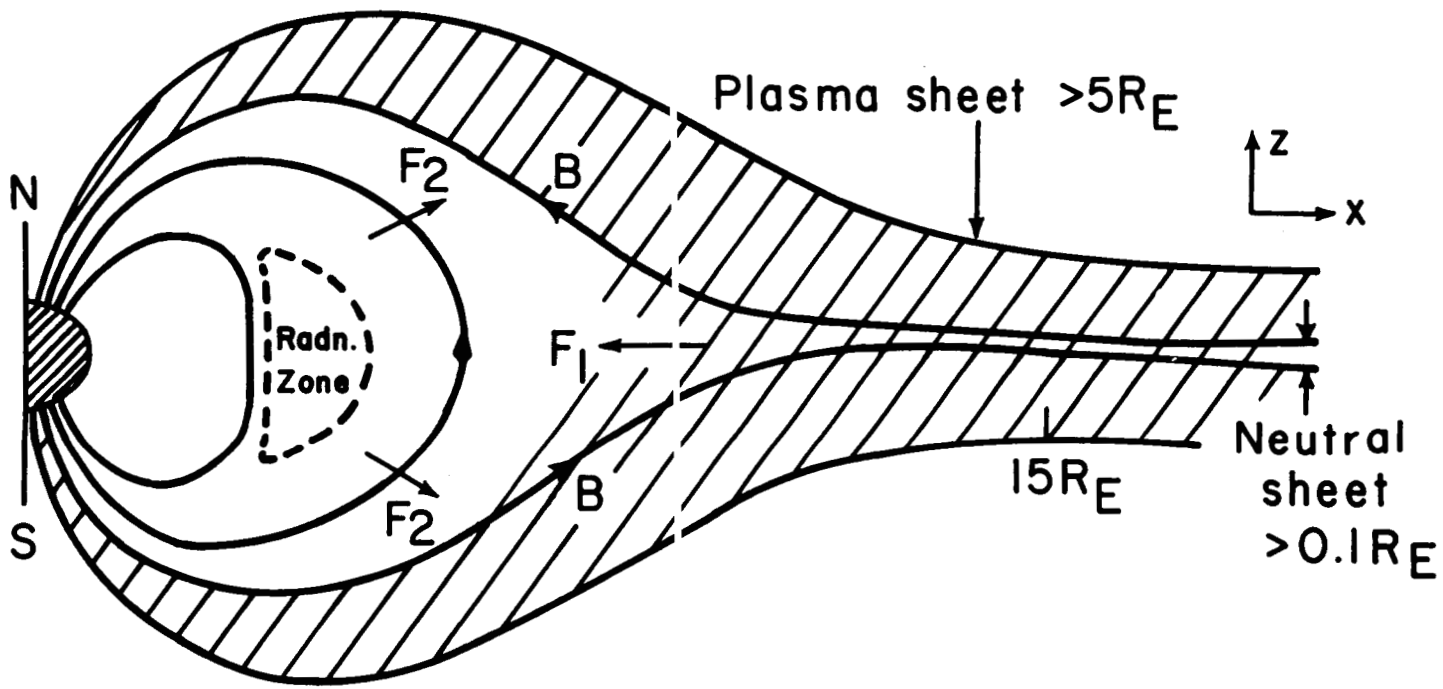
Plasma sheet >5R_E
z
x
N
S
F2
B
F1
Radn.
Zone
F2
B
15R_E
Neutral
sheet
>0.1R_E

F g. 4

G67 - 1034

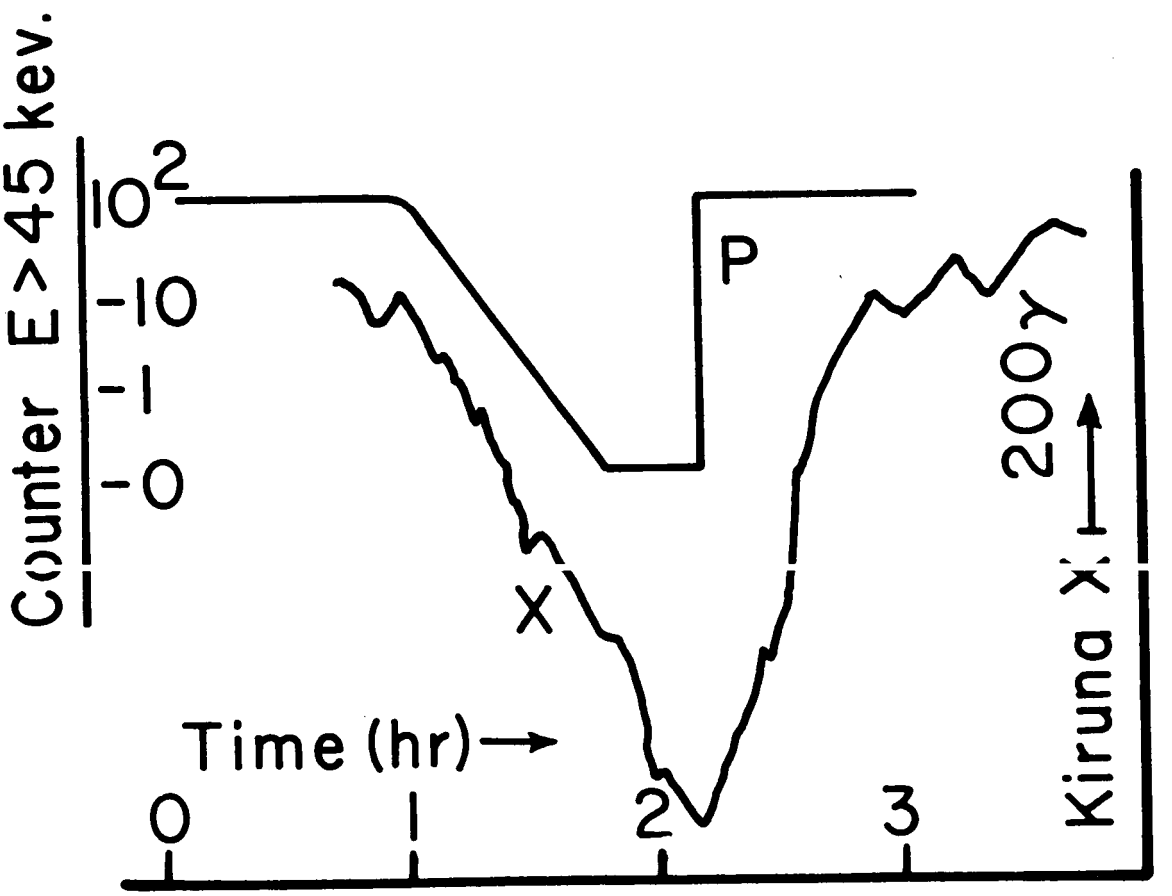

Fig. 5a

G67 - 1113

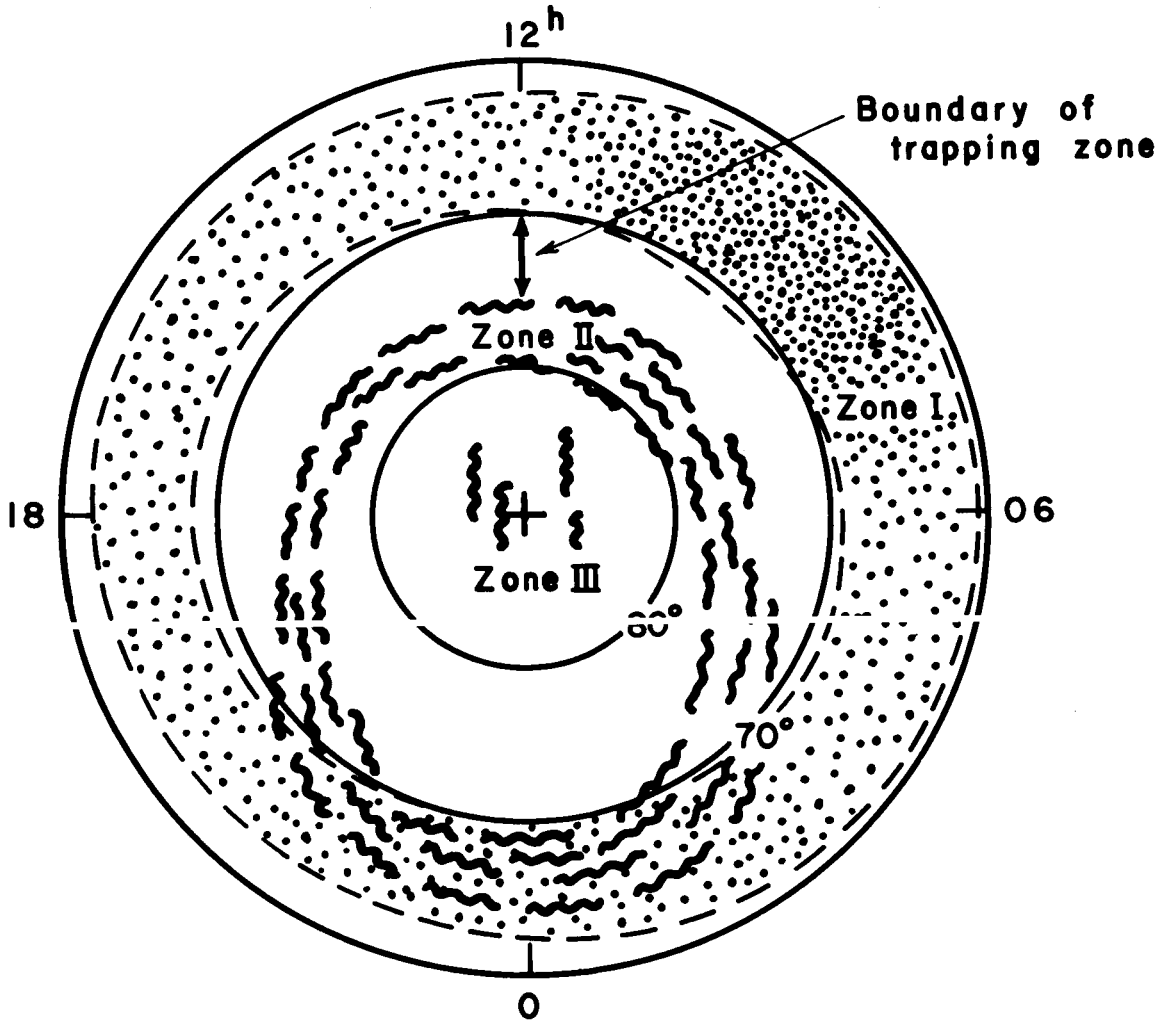

Fig. 5b

G67-1035

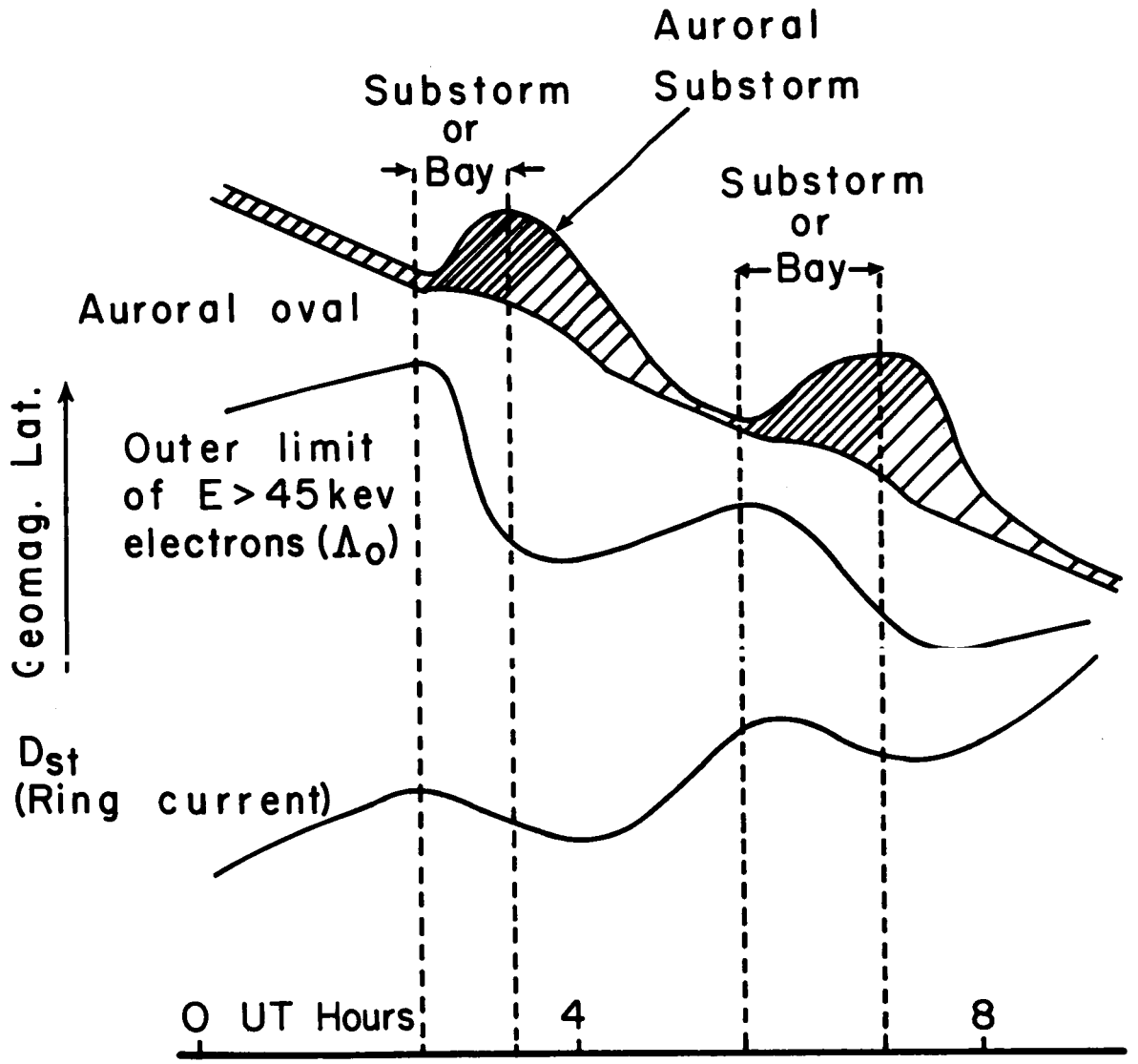

Fig. 6